A modelling approach in evaluating the effect of climate and LULC on groundwater level of Cochin, Kerala, India

Archana M Nair and Ande Bhuvaneswari

1. Introduction

The aquifer recharge process is complex and is influenced by climate conditions, LULC dynamics, aquifer lithology, and topography (Melki et al., 2017). As precipitation fluctuates with climate change due to temperature and evapotranspiration, there is a likelihood of discrepancy in groundwater recharge (Kahsay et al., 2018; Moeck et al., 2020). The amount of soil infiltration and deeper percolation is directly influenced by climate changes, which affect the groundwater recharge in the hydrological cycle (Shrestha et al., 2016; Wu et al., 2020). Similarly, alterations in LULC features are likely to have consequences on natural groundwater recharge systems since they alter the hydrological characteristics (Adhikari et al., 2020). The urbanisation-induced LULC changes lead to the rise in impervious surface coverage. More surface runoff indirectly causes a decrease in infiltration and a significant decline in groundwater recharge rates (A. M. Nair et al., 2016; Nath et al., 2021).

Kerala, a southern state in India, has experienced a higher accelerated economic development than the other states because of its geographical position, physical surroundings and socio-economic settings (Bindu and Mohamed, 2016). Mishra and Shah (2018) investigated the role of climate change and LULC changes on 2018-year floods in Kerala in their study. Pullare et al. (2015) stated that the recent developments in urbanisation, land use shifts, and cropping practices can reduce natural recharge into aquifers and increase groundwater extraction, affecting the state's groundwater situation. Thus, there is a necessity to understand the observed and projected impacts of climate and LULC change for the sustainable management of groundwater resources. The Ernakulum district, the business and industrial hub of Kerala, is considered as the study area. This area has recently experienced a rapid urban sprawl; with large scale LULC changes (Dipson et al., 2015). In this context, Nair et al. (2016) conducted a study to analyse the effect of LULC changes on surface runoff, and it was found that an increase in the effective impervious area has resulted in a significant increase in runoff and the same is reflected in groundwater level.

Sreekesh et al. (2018) studied climate change-induced sea-level rise and its effect on groundwater quality in the Ernakulum district. They found groundwater quality deterioration due to saltwater intrusion. However, there is a lack of comprehended studies that can relate the effects of climate and LULC on groundwater in the study area irrespective of the knowledge that the climate and LULC change significantly impact groundwater recharge. Therefore, in the present study, groundwater recharge was quantified for the future in the context of LULC and climate changes using SWAT. Studies related to the successful implementation of the SWAT model in groundwater resource assessment by several researchers are evident in the previous studies of Abunada et al., 2021; Bailey et al., 2020; Sahoo et al., 2019; Zhang et al., 2016. Consequently, this study focuses on (1) investigation of the impact from LULC changes on groundwater recharge under past (1994), present (2020), and future (2045, 2073, and 2100) LULC scenarios, and (2) investigation of the influence of both LULC and climate change on groundwater recharge for GFDL-ESM2M_REGCM4-ESM2M_RegCM4 and IPSL-CM5A-LR_REGCM4-CM5A-LR_REGCM4 model-based climatic projections (Chanapathi and Thatikonda, 2020) under RCP 4.5 and 8.5 scenarios.

1.1 Study Area

The study area is the highly urbanised Greater Cochin, which covers a significant portion of the Ernakulum district of Kerala. The lowlands are situated along the western region, whereas the high lands lie along the eastern region. Most of the lowland is located below the maximum altitude of 6 m above mean sea level(amsl). The midland region elevation ranges from 6 m to 75 m amsl, and high land elevation above 160 m amsl. The area falls within the watershed of the Periyar river towards the North and Muvatupuzha river towards the south. Geologically, the study area consists of two major litho-units comprising of Precambrian metamorphosed rocks in the eastern part and unconsolidated coastal alluvium in the western part. The region consists of sand, silt, clay of the lagoon, backwater deposits, and shore deposits with alluvial formations along the coastal belt, Laterites, Charnockites, and Charnockite gneiss rocks along the eastern midland. The major soil groups in the study area are lateritic, riverine alluvium, and coastal alluvium. The lateritic soil is the most predominant soil occupied by the region towards the central part, while coastal alluvium occupying the coastal stretch, and river alluvium is restricted to the banks of rivers and its tributaries. About 30% of the study area is covered with built lands. Most of the built-up lands are from the low land regions, the midland part is more of forest and agricultural lands. The study area belongs to the tropical climate with an annual average rainfall of around 3300 mm year^{-1}. The average minimum and maximum temperatures are about 23.2°C and 31.4°C. The relative humidity is in the range of 64 to 87% in the morning hours and 68 to 89% in the evening hours. The monthly potential evapotranspiration (PET) varies from 9.45 to 15.92 cm (Aneesh et al., 2019).

Groundwater generally occurs under phreatic conditions in the coastal sediments. In the midland region, the weathered and fractured crystalline zone is the aquifers, in which groundwater occurs in a semi-confined to confined state (Sreekesh et al., 2018). Groundwater is the additional source of freshwater to many parts of the study area. The alluvium forms a possible phreatic aquifer, extensively exploited with a large number of dug Wells and filter point Wells (Bhosale and Kumar, 2002).

1.2 Material and Methodology

The study focuses on modelling the effect of climate and LULC changes on groundwater recharge for the past, present and future scenarios. The study was accomplished in three steps as follows. First step: setup of a base model for the study area, which includes calibration and validation of the model; second step: modelling the impact of LULC changes on groundwater recharge under past (1994), present (2020) and future (2045, 2073, and 2100) LULC scenarios using observed climate data of 1985-2020, and third step: modelling the combined impact of LULC and climate Data collection

The elementary model setup of SWAT requires specific input on basic climatic data, which includes data for temperature, wind speed, rainfall, solar radiation, relative humidity, and geospatial data comprising of digital elevation model (DEM), land use management and soil type. When represented as DEM, Earth's topography can be utilised to delineate the watershed, stream network, and topographic and geomorphological parameter estimation (Chanapathi et al., 2020). The DEM, acquired from Shuttle Radar Topography Mission (SRTM) (http://www.usgs.gov/) having 30m resolution, is used for the topographic information of the area .The same DEM was used in the generation of the slope map. Geotechnical characteristic resource’s map of Ernakulum district, Kerala state (scale 1: 250,000) was utilised to prepare the soil map of the study area

(Source: Geological Survey of India, 2012). About 74% of the study area is covered with the Lateritic soil group.

1.2.1 LULC classification and future projections

A series of Landsat imageries collected for 1994, 2008, 2015, and 2020 were used in the LULC map generation that represents the LULC transformation for the past thirty years. LULC map was prepared using the Maximum Likelihood supervised classification technique. Maximum Likelihood is one of the most popular and robust methods for LULC classification (Kantakumar and Neelamsetti, 2015; Rizvi et al., 2020; Yonaba et al., 2021). From the analysis of spectral signatures, five key LULC classes identified for the study area. The five LULC types include forest, water bodies, fallow lands, agricultural lands, and built uplands. The spatial pattern and distribution of the five LULC classes in the study area for 1994, 2008, 2015, and 2020 are shown

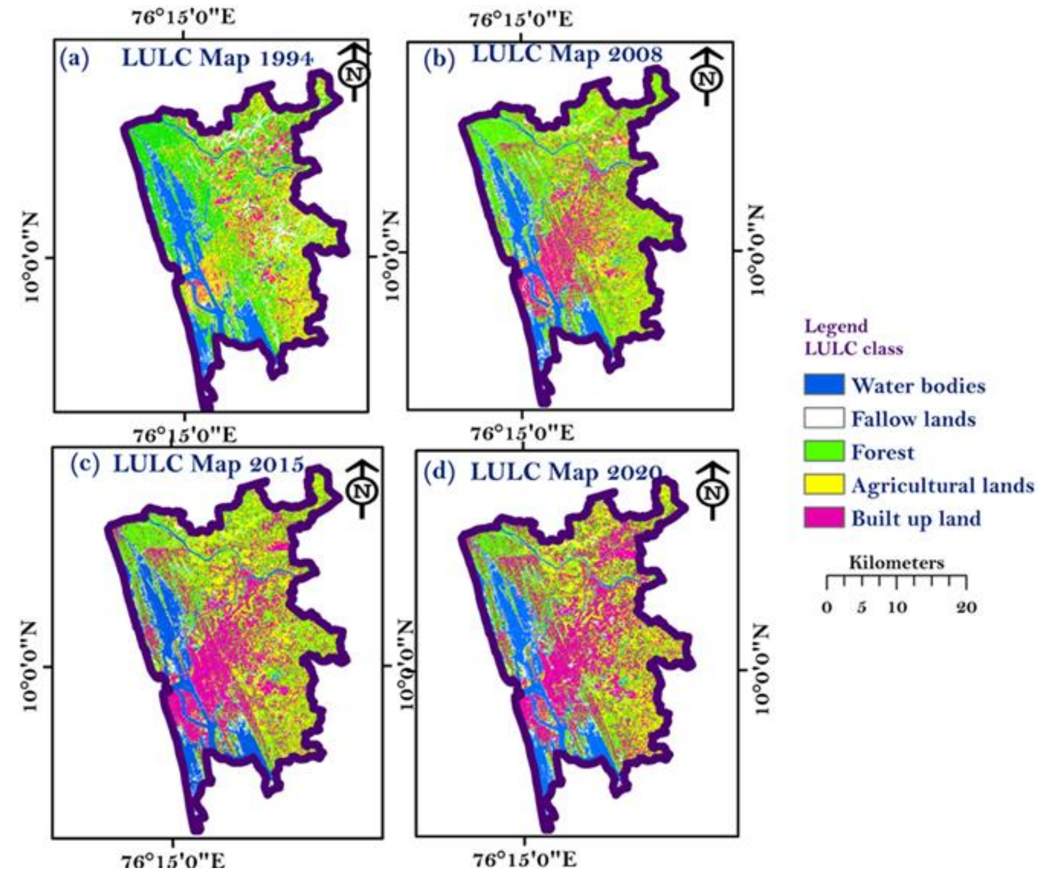

Figure 1 LULC maps of the study area (a) satellite-derived LULC maps of 1994, 2008. 2105 and 2020

in Fig 1a-d. The classification accuracy for each map was cross-checked with ground truth data separately. Agricultural lands occupied a substantial part of the study area, following the built-up lands and followed by the forest lands. The area under various LULC classes changed over the periods. Over the last three decades, a drastic increase in built-up lands was reported from the satellite-derived LULC maps represented in Fig. 1.

Various models such as CLUE–S (Lamichhane and Shakya, 2019), Land Change Modeller (LCM) (Yonaba et al., 2021), and Modules for Land Use Change Evaluation (MOLUSCE) (Habel et al., 2018), are available for future LULC prediction. For the present study, Modules for Land Use Change Evaluation (MOLUSCE) available in QGIS software was used for the LULC change analysis.

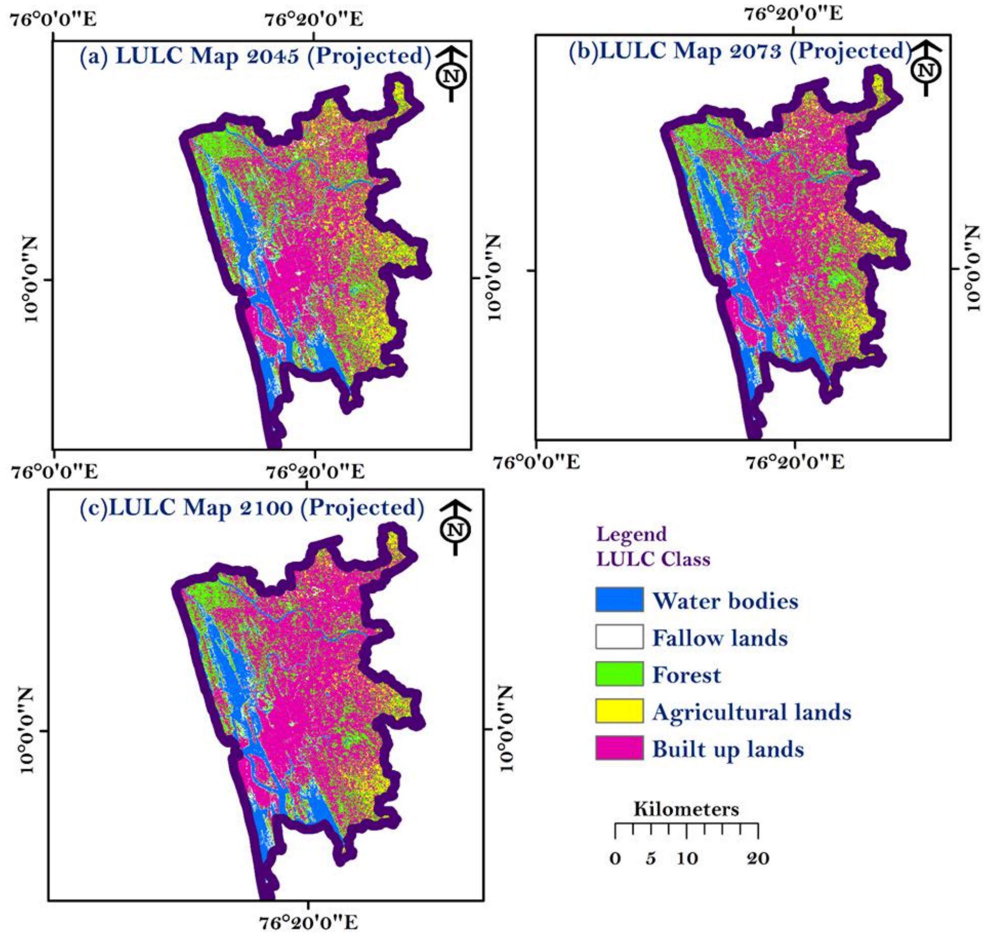

Figure 2 Projected LULC maps of (a) 2045, (b)2073, and (d)2100

In the study, satellite-derived LULC maps of 1994, 2008, 2015, and 2020 were used for the evaluation of model performance and for the projection of future LULC patterns over the study area. After the validation, the prediction of future LULC scenarios of 2045, 2073, and 2100 was carried out with the adopted model. The spatial distribution of simulated LULC future scenarios are represented in Fig. 2 a-c. LULC maps of 1994 and 2020 derived from satellite based remote sensing data were used in the SWAT model setup to represent the historical and present LULC scenario. Projected future LULC maps for 2045, 2073, and 2100 was used in the investigation of the impact of LULC changes on groundwater recharge in the future.

1.2.2 Climate Data and Models

Historical climate data such as precipitation with a spatial resolution of 0.25 degrees, maximum and minimum temperatures with a spatial resolution of 0.5 degrees were obtained daily for thirty-five years (1985 -2020) from the Indian Meteorological Department (IMD) Pune, India. This information formed the input for the model. The wind speed, relative humidity, and solar radiation were acquired from National Centres for Environmental Prediction (NCEP) Climate Forecast System Reanalysis (CFSR) website (http://globalweather.tamu.edu/) (Mechal et al., 2015; Sahoo et al., 2019) for the period 1985–2014 and were used for daily scale model setup. During the simulations, there is a connection established from every sub-basin to the nearest weather station. The model was set up for a warm-up period of 5 years from 1985, utilising a baseline period of 1990-2020. During the baseline period, the average annual precipitation was fixed as 3250 mm, T_{max} as 28.42, and T_{min} as 21.49. The wind speed was set between 0.8 km hr^{-1} to 10.1 km hr^{-1}, with a varied relative humidity from 50% to 89%.

The projected regional climate data for 1975 -2100 was downloaded from the existing Regional Climate Model (RCM) at South Asia CORDEX data portal (https://esgf-node.llnl.gov/search/esgf-llnl). RCM consider various socio-economic conditions to construct climate scenarios. GFDL-ESM2M_REGCM4-ESM2M_RegCM4, and IPSL-CM5A-LR_REGCM4-CM5A-LR_REGCM4 -CM5A-LR_RegCM4 models with 0.5° X 0.5° spatial resolution were utilised along with a daily time scale for Representative Concentration Pathway (RCP) 4.5 and RCP 8.5 scenarios. Three phases considered are Near Future (NF) for 2020-2045, Middle Future (MF) for 2046-2075, and Far Future (FF) for 2076-2100. Monthly streamflow data from 1999 to 2006 obtained for Ramamangalam gauge station (source: India-WRIS) was utilised to calibrate and validate the SWAT model.

1.2.3 Bias correction for future climate projection

GFDL-ESM2M_REGCM4-ESM2M_RegCM4 and IPSL-CM5A-LR_REGCM4-CM5A-LR_REGCM4 climate models were used to obtain the future climate data under the RCP 4.5 and 8.5 scenarios, as described above. Comparing simulated historical RCM data of precipitation and maximum or minimum temperature with observed IMD (India Meteorological Department) data has a substantial bias in RCM data, which emphasises the necessity for bias correction. The linear scaling approach is selected to eliminate biases from RCM in this study (Bhatta et al., 2019; Nilawar and Waikar, 2019). The linear scaling approach is a simple method that provides satisfactory error corrections. Here, the efficiency in correcting the errors in the RCM data for a daily time scale is determined from the difference between observed and simulated values (S. Shrestha et al., 2020). The simulated precipitation is adjusted with the multiplication factor depicted in Eq. (1) and (2), whereas temperature is adjusted with the additional factor as in Eq. (3) and (4).

$$P^{*}{}_{hist}\,(d) = P_{hist}(d) X \left[\frac{\mu_m\big(P_{obs}(d)\big)}{\mu_m\big(P_{hist}(d)\big)}\right] - - - - - (1)$$

$$P^{*}{}_{Simu}\,(d) = P_{Simu}(d) X \left[\frac{\mu_m\big(P_{obs}(d)\big)}{\mu_m\big(P_{hist}(d)\big)}\right] - - - - - (2)$$

$$T^{*}{}_{hist}\,(d) = T_{hist}(d) + \left[\mu_m\big(T_{obs}(d) - \mu_m T_{hist}(d)\big)\right] - - - - - (3)$$

$$T^{*}{}_{Simu}\,(d) = T_{Simu}(d) + \left[\mu_m\big(T_{obs}(d) - \mu_m T_{hist}(d)\big)\right] - - - - - (4)$$

where, P = precipitation, T = temperature, d = daily, μ_m = monthly mean, * = bias adjusted, hist = historical RCM data, obs = observed, simu = Raw RCM forecast.

1.2.4 SWAT hydrological model

Soil and Water Assessment Tool is a semi-distributed hydrological model that simulates the hydrologic responses in a continuous time-scale for a catchment (Arnold et al., 1998). The model has the capability of simulating spatiotemporal variation of groundwater (Zhang et al., 2016). Depending on the natural stream network and the DEM, the model delineates the entire watershed into several sub-basins which are further segmented into distinct hydrological response units (HRU). A specific combination of soil, slope, and land use make each HRU distinct. The water balance analysis for each HRU is computed in four distinct phases: snow, soil profile (<2 m), shallow (2-20 m), and deep aquifer (>20 m depth) (Narula and Gosain, 2013). The use of this process based model for multiple watersheds under different socio-economic development activities and environmental conditions enabled the evaluation of various aspects related to the studies on water resource management and water quality (Arnold et al., 1998; Dosdogru et al., 2020; Shrestha et al., 2021).

The recharge obtained from the SWAT model indicates the water that moves through the vadose zone, through the process of percolation or bypass flow from the bottom of soil profile further

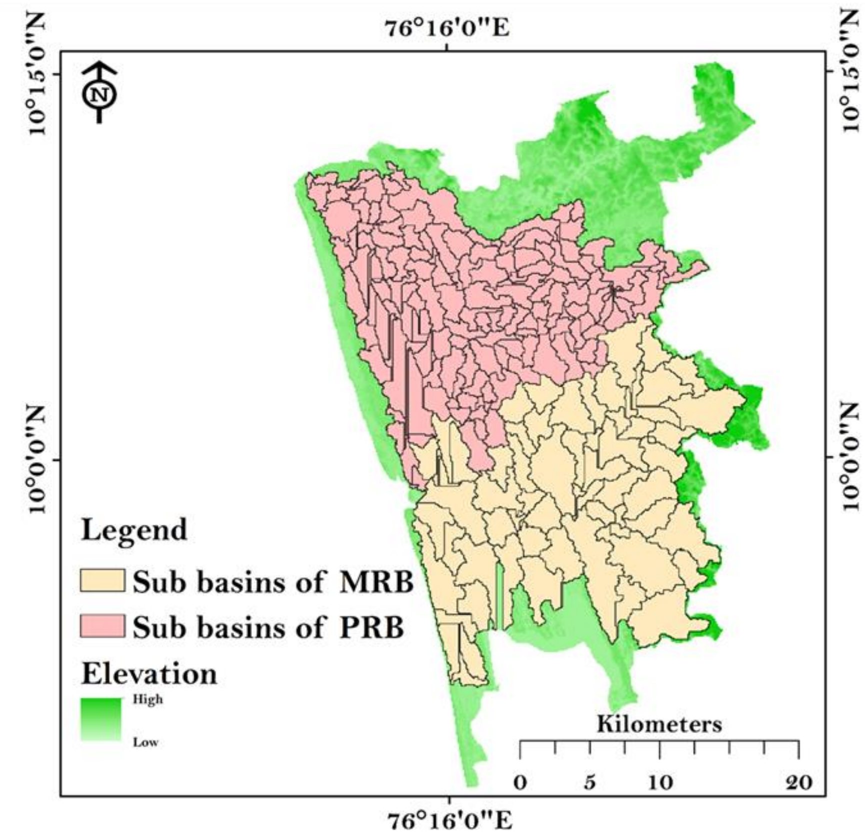

Figure 3 Sub basins of the Muvattupuzha and Periyar River Basins

(**MRB refers Muvattupuzha River Basins and PRB refers to Periyar River Basins)**

reaching the underlying aquifers (Gemitzi et al., 2017). The recharge to the unconfined shallow aquifer is subsidised by infiltration from the topsoil profile. In addition, there is a contribution of the base flow to the main channel or infiltration towards deeper aquifers by the recharge from the shallow aquifers (Dakhlalla et al., 2016; Gemitzi et al., 2017; Neitsch et al., 2011). The water balance equation used in the SWAT model for hydrological simulation is given in Eq. (6.5).

$$SW_t = SW_0 + \sum_{i=1}^{t}\left(P_{day} - Q_{Surf} - ET_a - W_{Seep} - Q_{surf}\right) - - - - - (6.5)$$

Where SW_t, SW_0 is the final and initial water content (mm) in day i, P_{day} amount of precipitation on day i (mm), Q_{Surf} amount of runoff (mm) on day i, ET_a amount of evapotranspiration (mm) on day i, W_{Seep} amount of water entering into the vadose zone from the soil profile (mm) on day i, and Q_{surf} is the amount base flow from shallow aquifer (mm) on day i.

In SWAT model, the study area was divided into numerous sub basins using the input DEM based on natural stream networks. Major watershed delineation for the study area using a threshold of 50 km^2 resulted in the demarcation of the Periyar watershed (300 km^2) and Muvattuphza watershed (350 km^2). A threshold of 5% of LULC, soil, and the slope was used to derive HRUs. A total of 2486 HRUs were defined for the study region within Periyar and Muvatupuzha watersheds. The model was simulated for a period of 35 years (1985-2020) which also includes the five years' warm-up period with observed data.

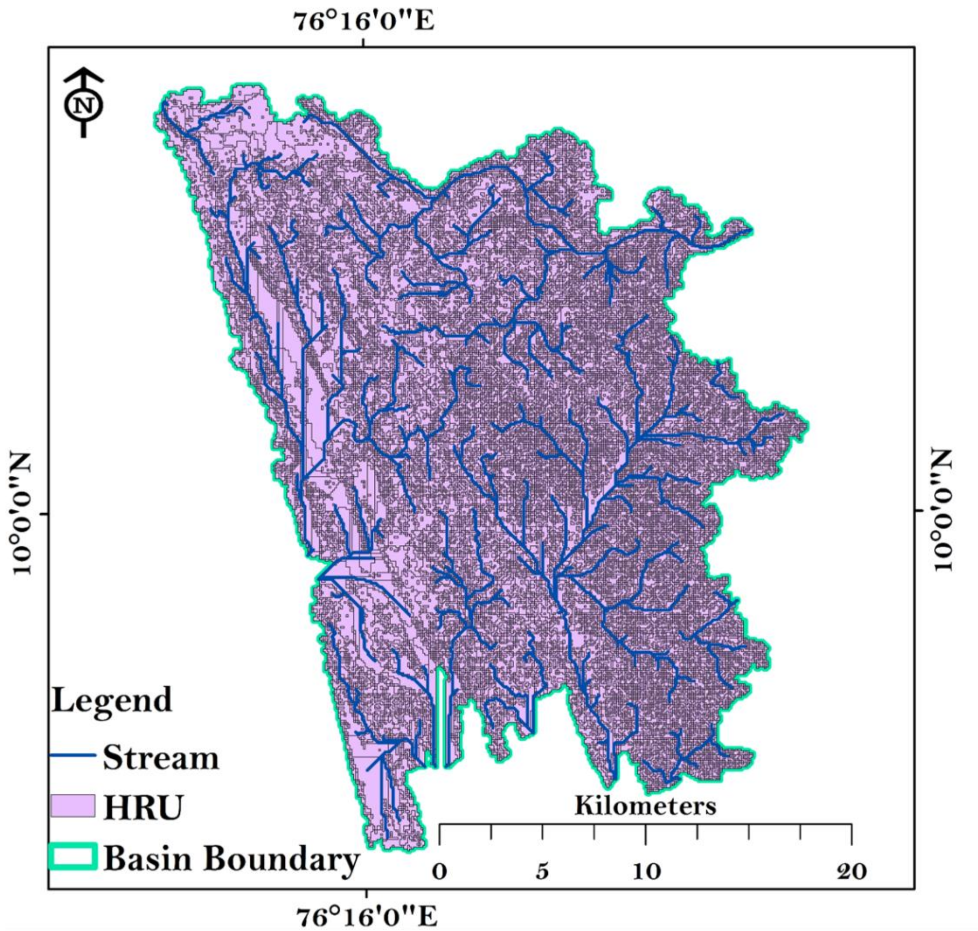

Figure 4 Discretisation of SWAT HRUs for MRB and PRB of the study area

1.2.5 Model Assessment

The model performance was evaluated based on thirteen SWAT parameters with Sequential Uncertainty Fitting Algorithm (SUFI2) approach, an auto-calibration program in SWAT-Calibration Uncertainty Programme (CUP). The coefficient of determination (R^2) and statistic operator Nash–Sutcliffe efficiency index (NSE) were utilised in the assessment of the model calibration and the validation at a monthly scale. Four years (1999-2003) of flow data for Periayer river at Ramamangalam was used for calibration, and four years (2003-2006) was utilised for validation. The model parameters selected for the calibration were modified within a predefined range during calibration to achieve the best agreement with the streamflow measurements (Gemitzi et al., 2017). Table 1 demonstrates the hydrological model parameters utilised for calibration and their fitted values. The LULC climate change impact on groundwater recharge was predicted with the calibrated SWAT model for future scenarios.

The performance of the model was assessed with the discharge data from 1999-2006 at Ramamangalam station. The sensitivity analysis in the calibration process was carried out to identify the sensitive parameters. Depending on the effect on the model outputs, sensitivity ranks were allotted to the model parameters. Twelve factors were selected for sensitivity investigation, out of which nine were identified to have high significance on model simulations (ALPH_BF.gw, CN2.mgt, EPCO.bsn, ESCO.bsn, RECHRG-DP.gw, GW_DELAY.gw, GW_REVAP.gw, CH_N2.rte, and GWQMN.gw), as reported in Table 1. Statistical performance indicators, R^2 and NSE indicators, calculated between observed and simulated streamflow values, were utilised to determine the accuracy of the simulations. The values of R^2 and NSE values were found to be 0.77 and 0.66 respectively for the calibration period, whereas for the validation, the values of R^2 value were found to be 0.68, and for NSE, the value was found to be 0.53. However, values greater than 0.5 designate satisfactory results for monthly calibration (Adhikary et al., 2019; Chanapathi and Thatikonda, 2020). Fig. 5 depicts the performance of model setup calibration and validation studies in the Ramamangalam gauge station. Further, in the following part, the influence of different LULC and climate scenarios were investigated with the calibrated SWAT model.

Table 1 Sensitivity analysis, their range of variability, and best-fitted values of the parameters

SWAT hydrological Parameter	**Parameter description**	**Parameter ranges**	**Fitted value**
ALPHA_BF.gw (v)	Base flow alpha factor (1/days)	[0, 1]	0.7
GW_DELAY.gw (v)	Delay time for aquifer recharge (days)	[0,500]	250
GWQMN.gw (v)	Threshold depth of water in shallow aquifer required for return flow to occur (mm)	[0,5000]	2500
GW_REVAP.gw (v)	Groundwater "revap" coefficient	[0.02,0.2]	0.11
RCHRG_DP.gw (v)	Deep aquifer percolation factor	[0,1]	0.5
REVAPMN.gw (v)	Threshold depth of water in shallow aquifer required for	[0,500]	50

	"revap" or percolation to deep aquifer to occur (mm)		
SOL_AWC ().sol (r)	Available water capacity of the soil layer	[-0.3,0.3]	0.12
SOL_K ().sol (r)	Saturated hydraulic conductivity (mm/h)	[-0.3,0.3]	0.12
ESCO.hru (v)	Soil evaporation compensation factor	[0,1]	0.9
CN2.mgt (r)	SCS runoff curve number	[-0.3 ,0.3]	0.069
CH_N2.rte (v)	Manning's "n" value for the main channel	[0.01, 0.3]	0.02
EPCO.hru (v)	Plant uptake compensation factor	[0,1]	0.7

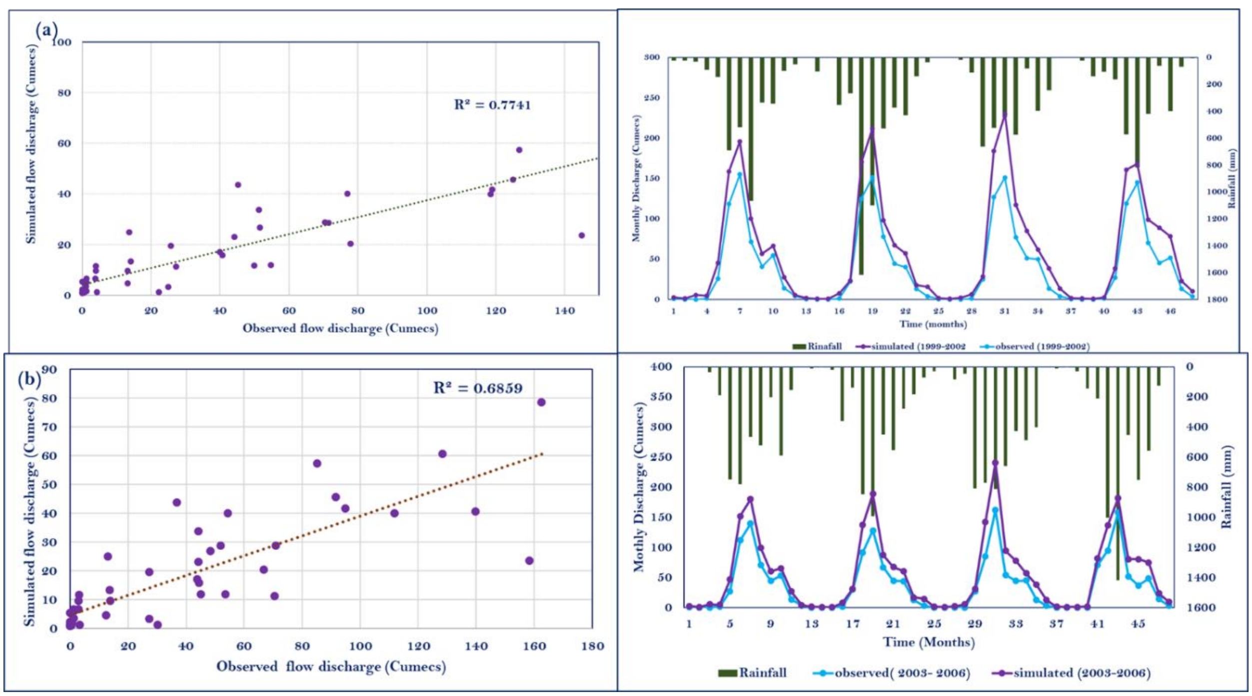

Figure 5 The calibration and validation graph using discharge data from the Ramamangalam gauge station

1.2.6 SWAT Model: Assessment of LULC change impact on groundwater recharge

Apart from the baseline period, few scenarios were set up to evaluate groundwater recharge due to the combined and individual effects of LULC, climate change. To analyse the LULC impact on the groundwater recharge, it was assumed that the future climate is similar to the baseline period (1985-2020). To assess the impact of LULC on recharge, we have three future simulated LULC scenarios at various time periods viz; 2045, 2073, and 2100. The model simulations were carried out under projected future LULC (2045, 2073, and 2100) data with historical climate data (1985-2020).

1.2.7 SWAT Model: Assessment of both LULC and climate change impact on groundwater recharge

Four phases with respect to climate, namely baseline (1985-2020), Near Future (2021-2045), Middle Future (2046-2075), and Far Future (2076-2100) were considered to analyse the combined impact of climate and LULC. The influence of both LULC and climate changes were evaluated with SWAT simulations. The projected LULC (2045, 2073, and 2100) with two RCM outputs of climate data for three different phases in the future viz., NF (2021-2045), MF (2046-2075), and FF (2076-2100)) for two RCP scenarios (RCP 4.5 and 8.5) were considered.

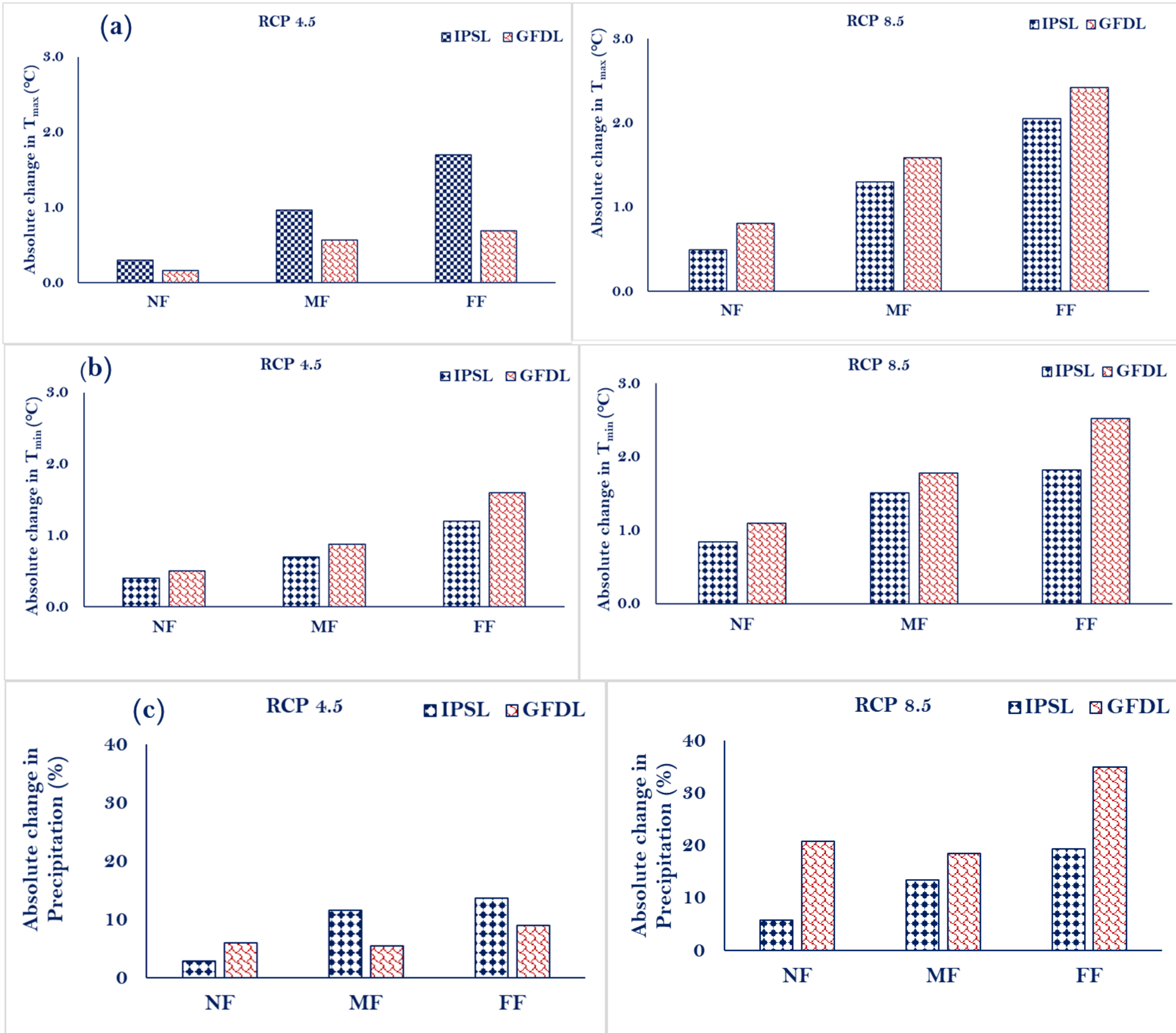

Figure 8 (a) Projected change in maximum temperature, (b) minimum temperature, and (c) precipitation for the three future periods: NF (2021–2045), MF (2046–2065), and FF (2076–2099) relative to the baseline period (1985–2020) under RCP 4.

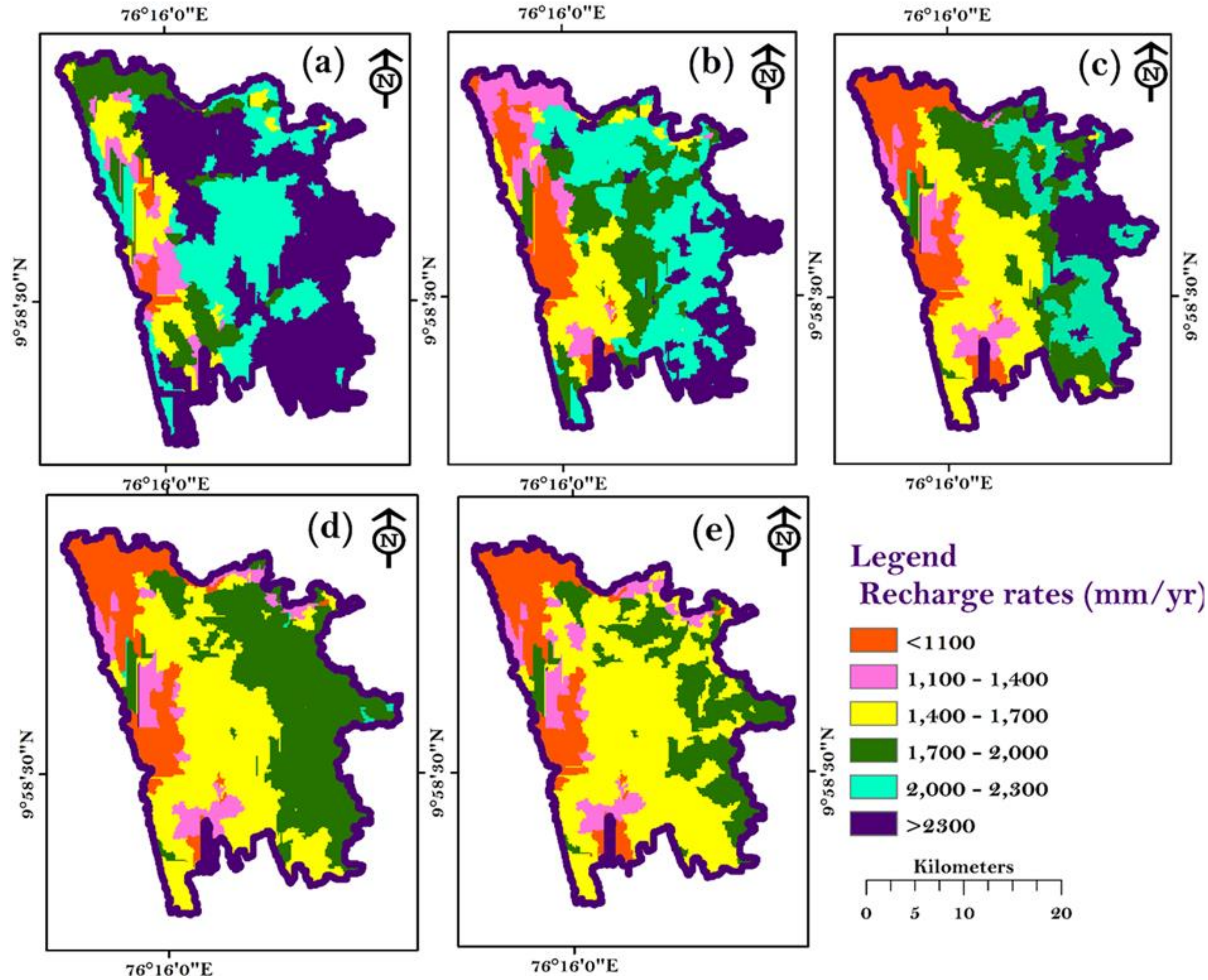

Figure 9 Simulated groundwater recharge rate maps; (a) under 1994 LULC, (b) under 2020 LULC, (c) under 2045 LULC, (d) under 2073 LULC, and (e) under 2100 LULC

The projected LULC from 1994 to 2100 demonstrates an expansion of urban land areas at the cost of natural land covers such as forest, agricultural lands, fallow lands, and water bodies. Therefore, a significant decrease in recharge rate is observed in the highly urbanised scenario (LULC 2100) compared to the baseline period. A negative trend observed in the forecasted average annual recharge rates could be attributed to the drastic increase in the impervious surface. The mean annual recharge rates showed a reduction to the 1994 mean annual recharge rate at 14%,

Table. 2 Spatial distribution statistics of simulated recharge depths for various LULC

	Spatial distribution (%) of simulated recharge under different LULC maps

Recharge Depth (mm yr^{-1})	1994	2020	2045	2073	2100
<1100	1.9	9.1	15.9	15.8	17.0
1100-1400	4.9	11.8	7.2	8.5	9.6
1400-1700	11.7	17.6	33.3	44.2	65.3
1700-2000	16.7	28.4	21.8	31.5	9.1
2000-2300	45.2	31.3	20.3	0.1	0.1
>2300	19.6	1.9	1.6	0.0	0.0

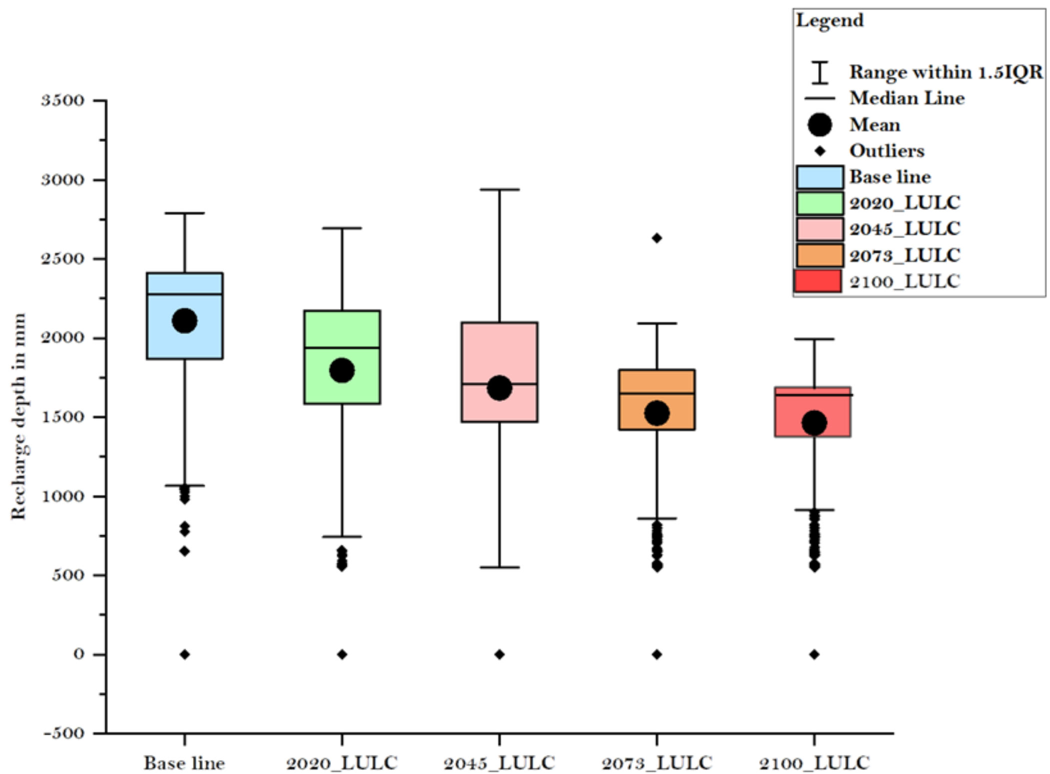

Figure 10 Comparison of mean simulated recharge rates under future scenarios with reference to baseline groundwater recharge rate (1994) for different LULC scenarios.

20%, 27%, and 30%, for LULC 2020, 2045, 2073, and 2100. It is observed that the distribution of the area covered with high recharge rates reduced tremendously in the future with a steady expansion of the area with low recharge rates (Table 2).

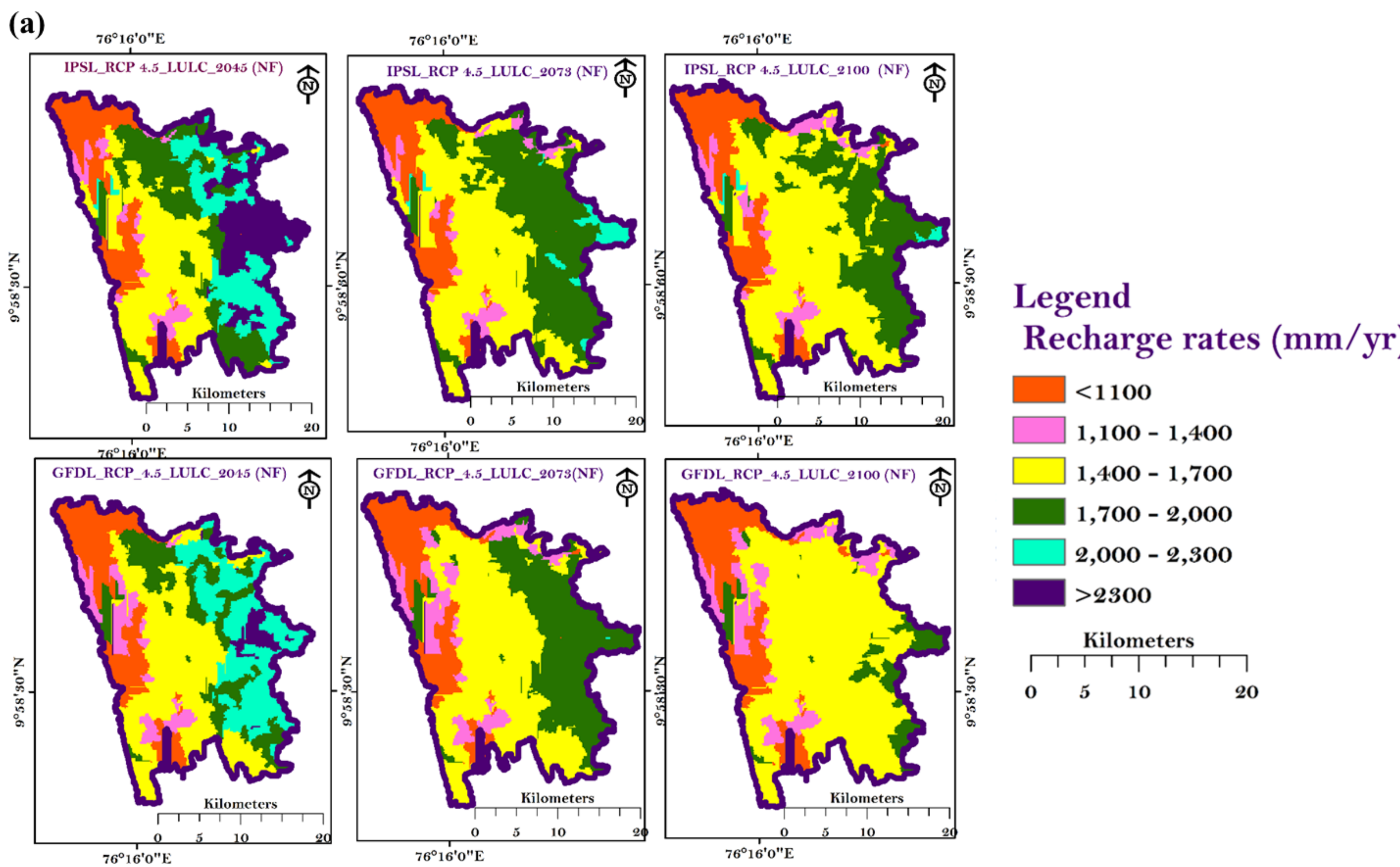

(a)
IPSL_RCP 4.5_LULC_2045 (NF)
IPSL_RCP 4.5_LULC_2073 (NF)
IPSL_RCP 4.5_LULC_2100 (NF)
GFDL_RCP_4.5_LULC_2045 (NF)
GFDL_RCP_4.5_LULC_2073(NF)
GFDL_RCP_4.5_LULC_2100 (NF)
76°16'0"E
9°58'30"N
Kilometers
0 5 10 20
Legend
Recharge rates (mm/yr)
<1100
1,100 - 1,400
1,400 - 1,700
1,700 - 2,000
2,000 - 2,300
>2300

(b)

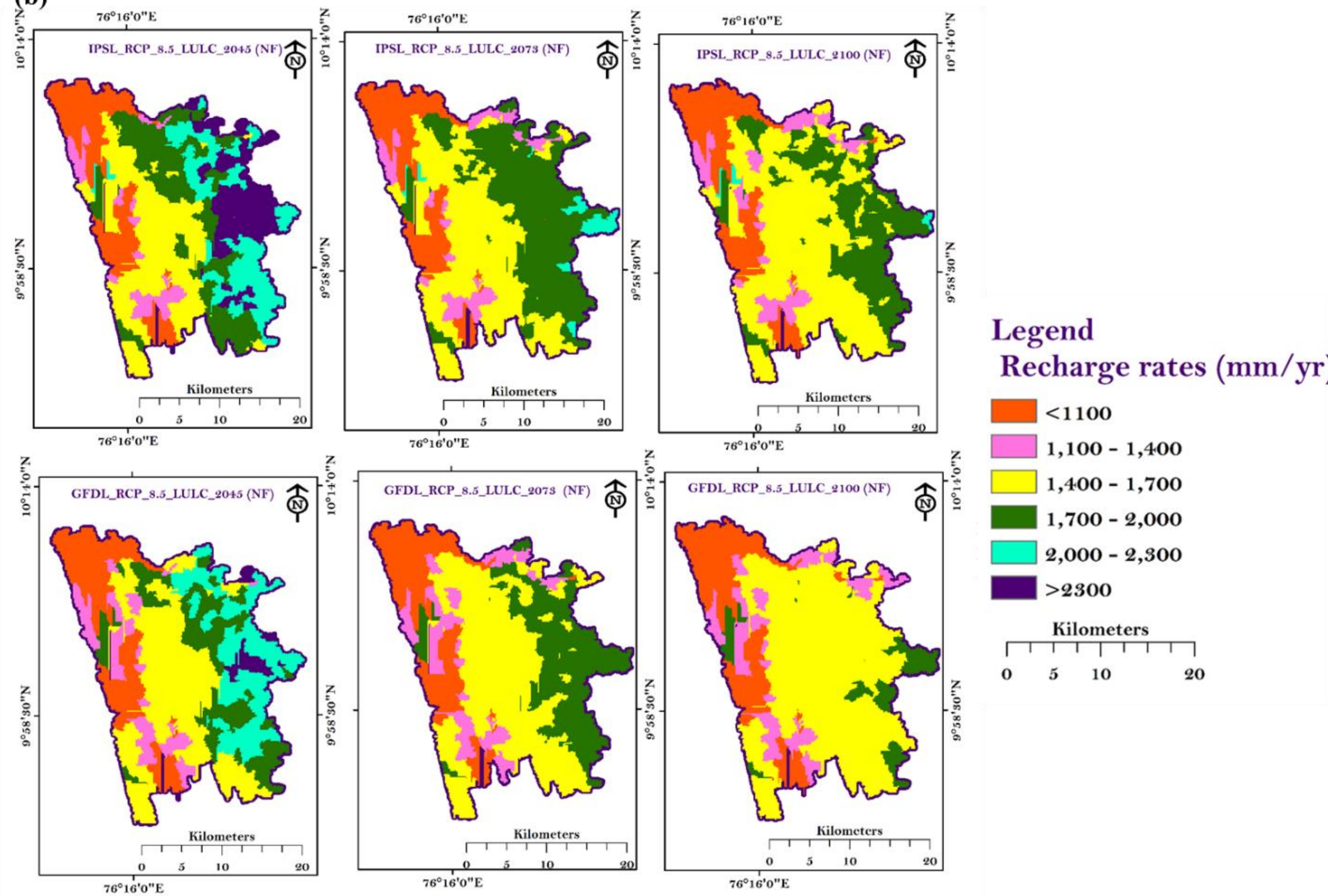

IPSL_RCP_8.5_LULC_2045 (NF)
IPSL_RCP_8.5_LULC_2073 (NF)
IPSL_RCP_8.5_LULC_2100 (NF)
GFDL_RCP_8.5_LULC_2045 (NF)
GFDL_RCP_8.5_LULC_2073 (NF)
GFDL_RCP_8.5_LULC_2100 (NF)
76°16'0"E
10°14'0"N
9°58'30"N
N
Kilometers
0 5 10 20
Legend
Recharge rates (mm/yr)
<1100
1,100 - 1,400
1,400 - 1,700
1,700 - 2,000
2,000 - 2,300
>2300

(c)

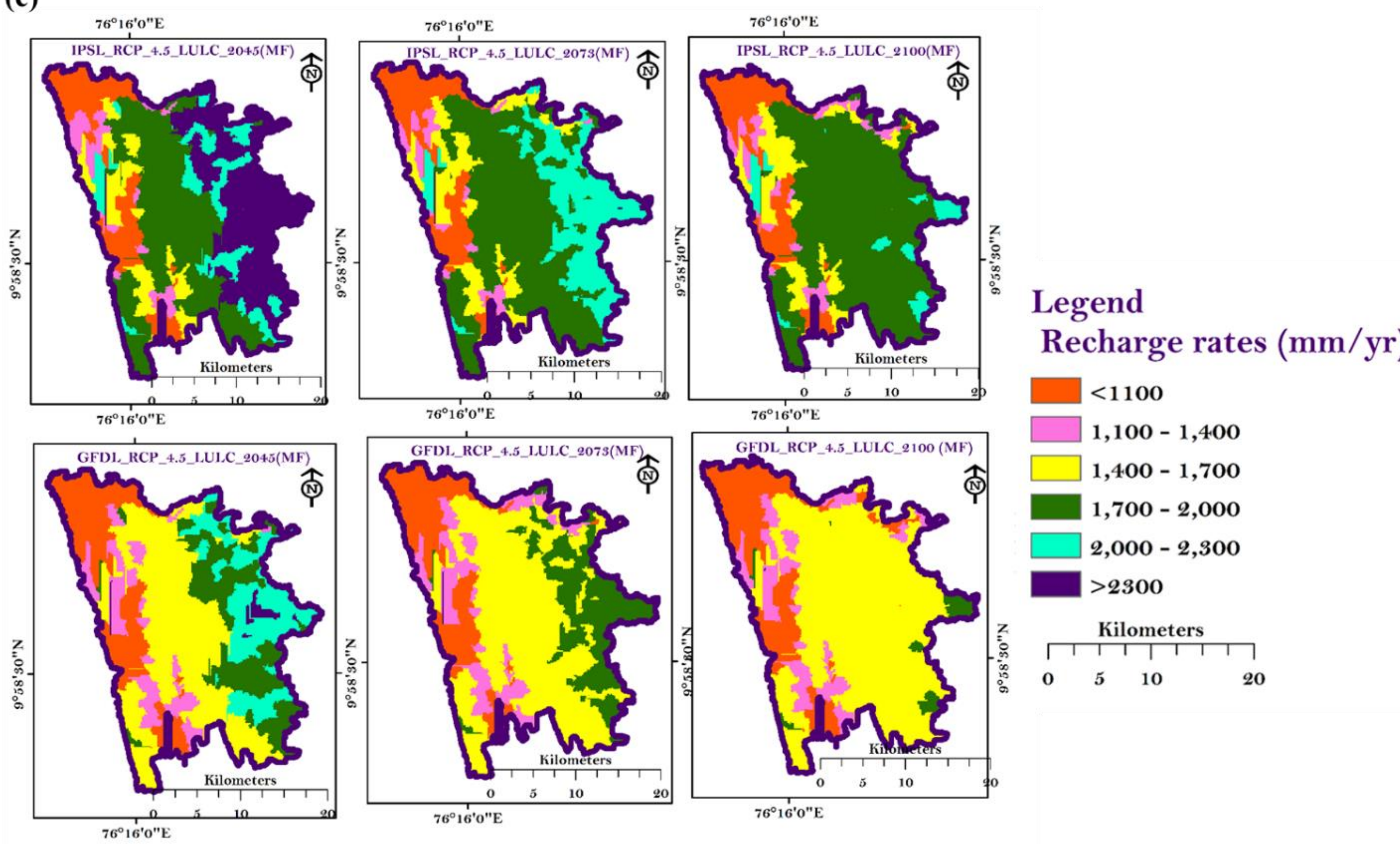
IPSL_RCP_4.5_LULC_2045(MF)
IPSL_RCP_4.5_LULC_2073(MF)
IPSL_RCP_4.5_LULC_2100(MF)
GFDL_RCP_4.5_LULC_2045(MF)
GFDL_RCP_4.5_LULC_2073(MF)
GFDL_RCP_4.5_LULC_2100 (MF)
76°16'0"E
9°58'30"N
Kilometers
0 5 10 20
Legend
Recharge rates (mm/yr)
<1100
1,100 - 1,400
1,400 - 1,700
1,700 - 2,000
2,000 - 2,300
>2300

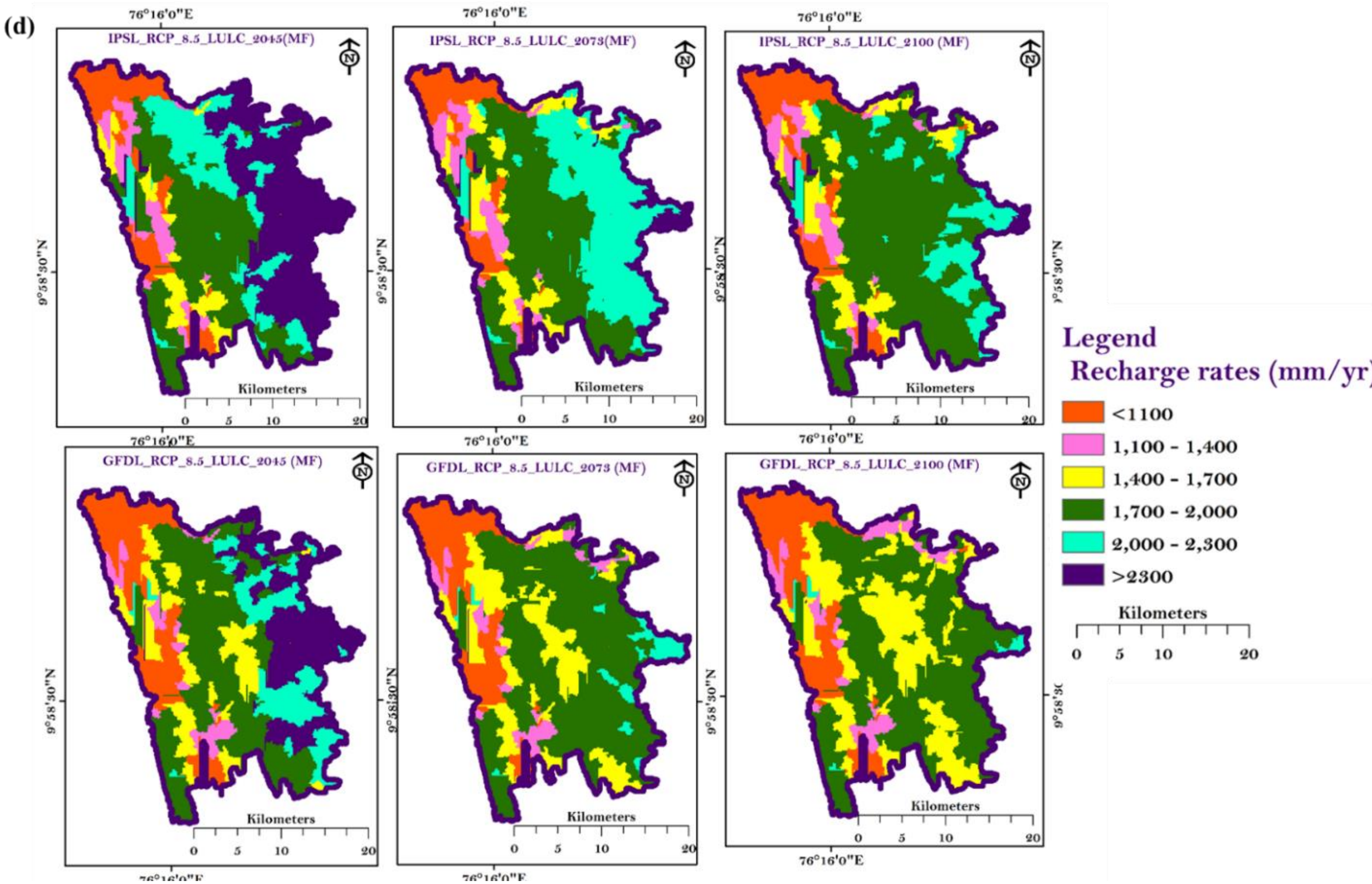

(d)
IPSL_RCP_8.5_LULC_2045(MF)
IPSL_RCP_8.5_LULC_2073(MF)
IPSL_RCP_8.5_LULC_2100 (MF)
GFDL_RCP_8.5_LULC_2045 (MF)
GFDL_RCP_8.5_LULC_2073 (MF)
GFDL_RCP_8.5_LULC_2100 (MF)
76°16'0"E
9°58'30"N
Kilometers
0 5 10 20
Legend
Recharge rates (mm/yr)
<1100
1,100 - 1,400
1,400 - 1,700
1,700 - 2,000
2,000 - 2,300
>2300

(e)

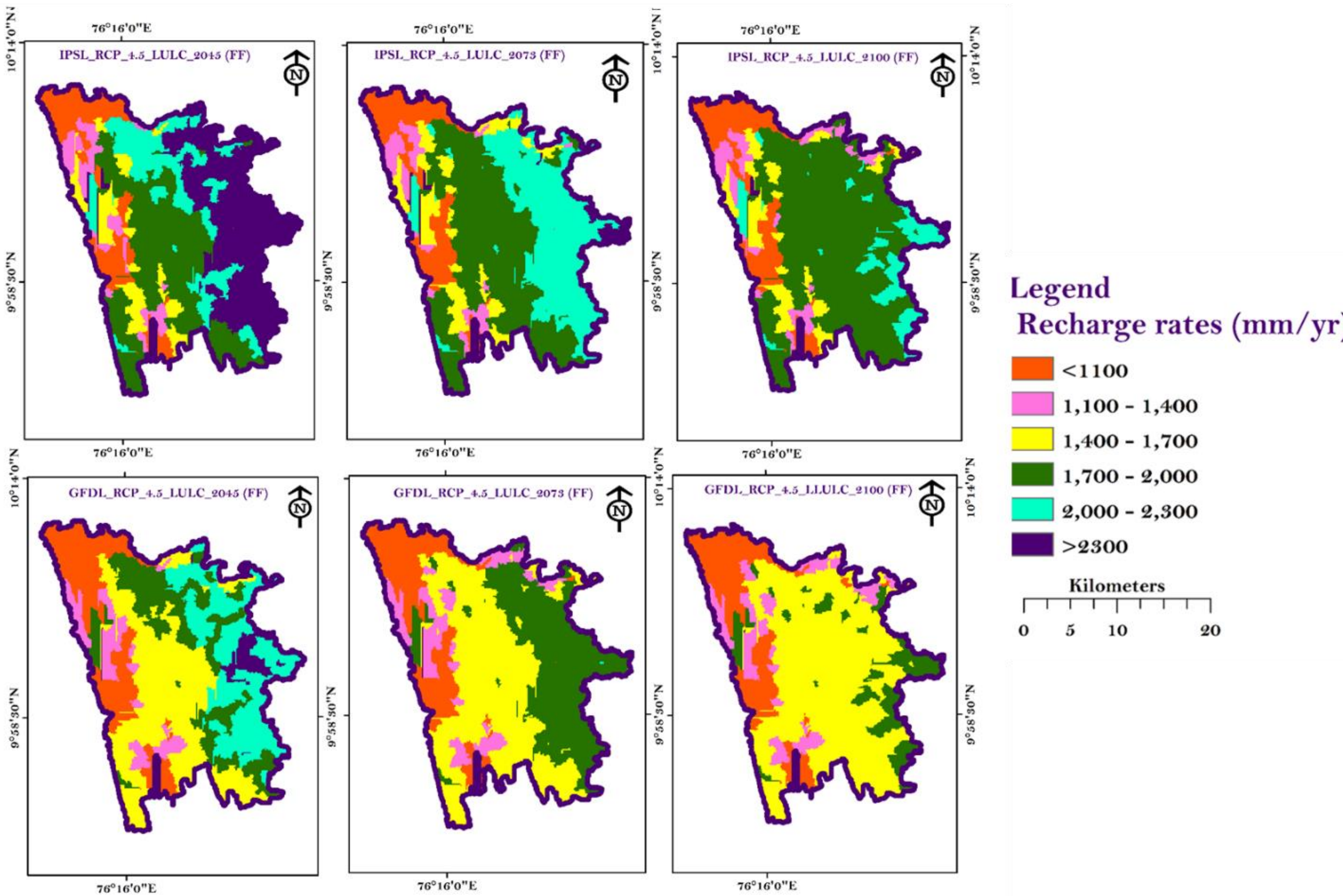

IPSL_RCP_4.5_LULC_2045 (FF)
IPSL_RCP_4.5_LULC_2073 (FF)
IPSL_RCP_4.5_LULC_2100 (FF)
GFDL_RCP_4.5_LULC_2045 (FF)
GFDL_RCP_4.5_LULC_2073 (FF)
GFDL_RCP_4.5_LLULC_2100 (FF)
76°16'0"E
10°14'0"N
9°58'30"N
N
Legend
Recharge rates (mm/yr)
<1100
1,100 - 1,400
1,400 - 1,700
1,700 - 2,000
2,000 - 2,300
>2300
Kilometers
0 5 10 20

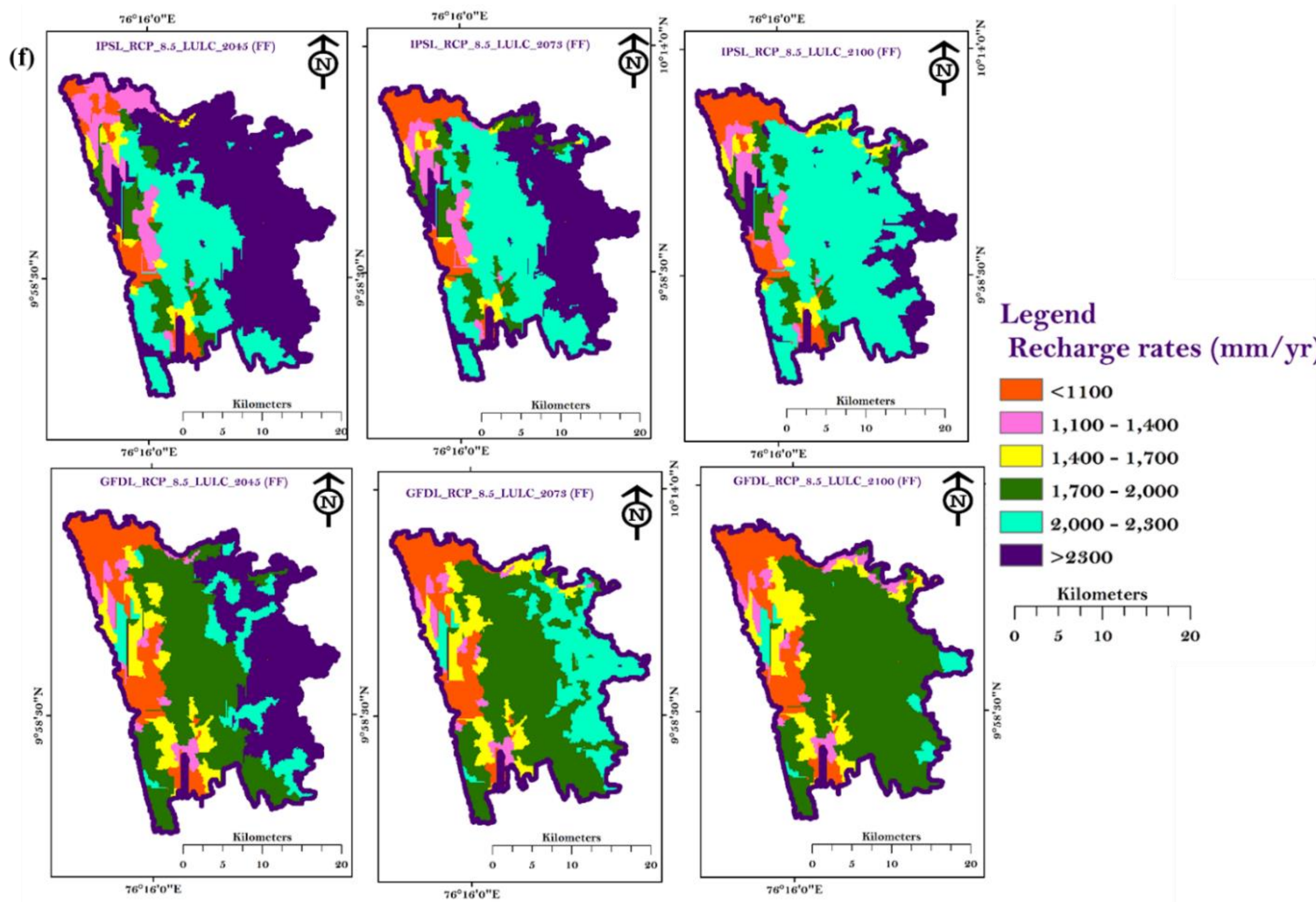

Figure 11 Spatial distribution groundwater recharge rate for various LULC and climate change under RCP 4.5 and 8.5 scenarios under various LULC (2045, 2073, and 2100) (a) for near future (NF) under RCP 4.5 (b) for near future (NF) under RCP 8.5, (c) for middle future (MF) under RCP 4.5, (d) for middle future (MF) under RCP 8.5, (e) for far future (FF) under RCP 4.5), and (f) for far future (FF) under RCP 8.5

Table 3 Projected groundwater recharge rates (%) for a combination of Climate and LULC scenarios

Scenario 1: Projected climate data from IPSL-CM5A-LR_REGCM4-CM5A-LR_REGCM4 RCP 4.5 Near Future (2021-2045)				
LULC scenarios	**Case 1** **Base line**	**Case 2**	**Case 3**	**Case 4**
	Observed LULC 1994	**Forecasted Future LULC 2045**	**Forecasted Future LULC** **2073**	**Forecasted Future LULC** **2100**
Recharge rates in mm/year				
<1100	1.88	15.19	14.73	15.92
1100-1400	4.92	5.27	6.22	7.77
1400-1700	11.68	30.58	40.31	54.43
1700-2000	16.75	22.48	38.23	22.94
2000-2300	45.16	23.33	0.53	0.09
>2300	19.58	3.22	0.00	0.00
Scenario 2: Projected climate data from GFDL-ESM2M_REGCM4-ESM2M_RegCM4 RCP 4.5 Near Future (2021-2045)				
LULC scenarios	**Case 1** **Base line**	**Case 2**	**Case 3**	**Case 4**
	Observed LULC 1994	**Forecasted Future LULC 2045**	**Forecasted Future LULC** **2073**	**Forecasted Future LULC** **2100**
Recharge rates in mm/year				
<1100	1.88	16.27	16.19	17.53
1100-1400	4.92	8.30	10.88	11.38
1400-1700	11.68	39.22	51.58	68.29
1700-2000	16.75	18.80	21.47	3.95

2000-2300	45.16	16.63	0.00	0.00
>2300	19.58	0.84	0.00	0.00
Scenario 3: Projected climate data from IPSL-CM5A-LR_REGCM4-CM5A-LR_REGCM4 RCP 8.5 Near Future (2021-2045)				
LULC scenarios	**Case 1** **Base line**	**Case 2**	**Case 3**	**Case 4**
	Observed LULC 1994	**Forecasted Future LULC 2045**	**Forecasted Future LULC** **2073**	**Forecasted Future LULC** **2100**
Recharge rates in mm/year				
<1100	1.88	15.19	14.73	15.92
1100-1400	4.92	6.48	7.99	9.25
1400-1700	11.68	32.16	42.44	61.13
1700-2000	16.75	20.29	34.52	14.76
2000-2300	45.16	22.73	0.35	0.09
>2300	19.58	3.22	0.00	0.00
Scenario 4: Projected climate data from GFDL-ESM2M_REGCM4-ESM2M_RegCM4 RCP 8.5 Near Future (2021-2045)				
LULC scenarios	**Case 1** **Base line**	**Case 2**	**Case 3**	**Case 4**
	Observed LULC 1994	**Forecasted Future LULC 2045**	**Forecasted Future LULC** **2073**	**Forecasted Future LULC** **2100**
Recharge rates in mm/year				
<1100	1.88	14.05	17.03	18.33
1100-1400	4.92	5.33	11.88	12.93
1400-1700	11.68	10.25	54.45	66.86
1700-2000	16.75	38.90	16.67	3.03

2000-2300	45.16	13.54	0.00	0.00
>2300	19.58	17.99	0.00	0.00
Scenario 5: Projected climate data from IPSL-CM5A-LR_REGCM4-CM5A-LR_REGCM4 RCP 4.5 Middle Future (2046-2075)				
LULC scenarios	**Case 1** **Base line**	**Case 2**	**Case 3**	**Case 4**
	Observed LULC 1994	**Forecasted Future LULC 2045**	**Forecasted Future LULC 2073**	**Forecasted Future LULC** **2100**
Recharge rates in mm/year				
<1100	1.88	11.86	12.42	14.16
1100-1400	4.92	7.23	6.11	7.38
1400-1700	11.68	10.35	13.26	13.42
1700-2000	16.75	39.10	59.78	64.23
2000-2300	45.16	14.06	8.55	1.96
>2300	19.58	17.47	0.00	0.00
Scenario 6: Projected climate data from GFDL-ESM2M_REGCM4-ESM2M_RegCM4 RCP 4.5 Middle Future (2046-2075)				
LULC scenarios	**Case 1** **Base line**	**Case 2**	**Case 3**	**Case 4**
	Observed LULC 1994	**Forecasted Future LULC 2045**	**Forecasted Future LULC 2073**	**Forecasted Future LULC** **2100**
Recharge rates in mm/year				
<1100	1.88	17.42	17.32	18.62
1100-1400	4.92	10.43	12.39	13.28
1400-1700	11.68	40.55	61.24	67.51
1700-2000	16.75	19.87	9.08	1.74

2000-2300	45.16	11.36	0.00	0.00
>2300	19.58	0.43	0.00	0.00
Scenario 7: Projected climate data from IPSL-CM5A-LR_REGCM4-CM5A-LR_REGCM4 RCP 8.5 Middle Future (2046-2075)				
LULC scenarios	**Case 1** **Base line**	**Case 2**	**Case 3**	**Case 4**
	Observed LULC 1994	**Forecasted Future LULC 2045**	**Forecasted Future LULC 2073**	**Forecasted Future LULC 2100**
Recharge rates in mm/year				
<1100	1.88	9.29	11.06	12.18
1100-1400	4.92	7.79	6.38	6.56
1400-1700	11.68	10.06	11.83	12.73
1700-2000	16.75	35.14	46.77	62.89
2000-2300	45.16	11.65	23.63	6.79
>2300	19.58	26.13	0.35	0.00
Scenario 8: Projected climate data from GFDL-ESM2M_REGCM4-ESM2M_RegCM4 RCP 8.5 Middle Future (2046-2075)				
LULC scenarios	**Case 1** **Base line**	**Case 2**	**Case 3**	**Case 4**
	Observed LULC 1994	**Forecasted Future LULC 2045**	**Forecasted Future LULC 2073**	**Forecasted Future LULC 2100**
Recharge rates in mm/year				
<1100	1.88	15.19	14.73	6.13
1100-1400	4.92	5.63	6.58	7.77
1400-1700	11.68	28.58	39.27	51.88
1700-2000	16.75	22.84	38.70	25.49

2000-2300	45.16	17.88	0.75	0.09
>2300	19.58	9.96	0.00	0.00
Scenario 9: Projected climate data from IPSL-CM5A-LR_REGCM4-CM5A-LR_REGCM4 RCP 4.5 Far Future (2076-2100)				
LULC scenarios	**Case 1** **Base line**	**Case 2**	**Case 3**	**Case 4**
	Observed LULC 1994	**Forecasted Future LULC 2045**	**Forecasted Future LULC 2073**	**Forecasted Future LULC** **2100**
Recharge rates in mm/year				
<1100	1.88	11.00	11.06	12.18
1100-1400	4.92	7.43	7.12	8.88
1400-1700	11.68	9.28	11.48	10.81
1700-2000	16.75	36.24	50.27	65.59
2000-2300	45.16	13.98	20.01	3.69
>2300	19.58	22.12	0.09	0.00
Scenario 10: Projected climate data from GFDL-ESM2M_REGCM4-ESM2M_RegCM4 RCP 4.5 Far Future (2076-2100)				
LULC scenarios	**Case 1** **Base line**	**Case 2**	**Case 3**	**Case 4**
	Observed LULC 1994	**Forecasted Future LULC 2045**	**Forecasted Future LULC 2073**	**Forecasted Future LULC** **2100**
Recharge rates in mm/year				
<1100	1.88	16.45	16.19	17.53
1100-1400	4.92	8.12	10.61	11.38
1400-1700	11.68	37.72	49.27	67.13
1700-2000	16.75	20.30	23.86	5.11

2000-2300	45.16	16.63	0.09	0.00
>2300	19.58	0.84	0.00	0.00
Scenario 11: Projected climate data from IPSL-CM5A-LR_REGCM4-CM5A-LR_REGCM4 RCP 8.5 Far Future (2076-2100)				
LULC scenarios	**Case 1** **Base line**	**Case 2**	**Case 3**	**Case 4**
	Observed LULC 1994	**Forecasted Future LULC 2045**	**Forecasted Future LULC 2073**	**Forecasted Future LULC** **2100**
Recharge rates in mm/year				
<1100	1.88	4.40	7.21	8.65
1100-1400	4.92	10.77	8.00	7.93
1400-1700	11.68	4.45	3.85	5.87
1700-2000	16.75	9.54	12.54	12.10
2000-2300	45.16	34.14	49.66	62.22
>2300	19.58	36.77	18.77	4.36
Scenario 12: Projected climate data from GFDL-ESM2M_REGCM4-ESM2M_RegCM4 RCP 8.5 Far Future (2076-2100)				
LULC scenarios	**Case 1** **Base line**	**Case 2**	**Case 3**	**Case 4**
	Observed LULC 1994	**Forecasted Future LULC 2045**	**Forecasted Future LULC 2073**	**Forecasted Future LULC 2100**
Recharge rates in mm/year				
<1100	1.88	14.05	14.10	15.30
1100-1400	4.92	5.33	4.72	6.25
1400-1700	11.68	10.25	13.88	13.42
1700-2000	16.75	38.90	60.55	64.84
2000-2300	45.16	13.54	6.77	1.35

>2300	19.58	17.99	0.00	0.00

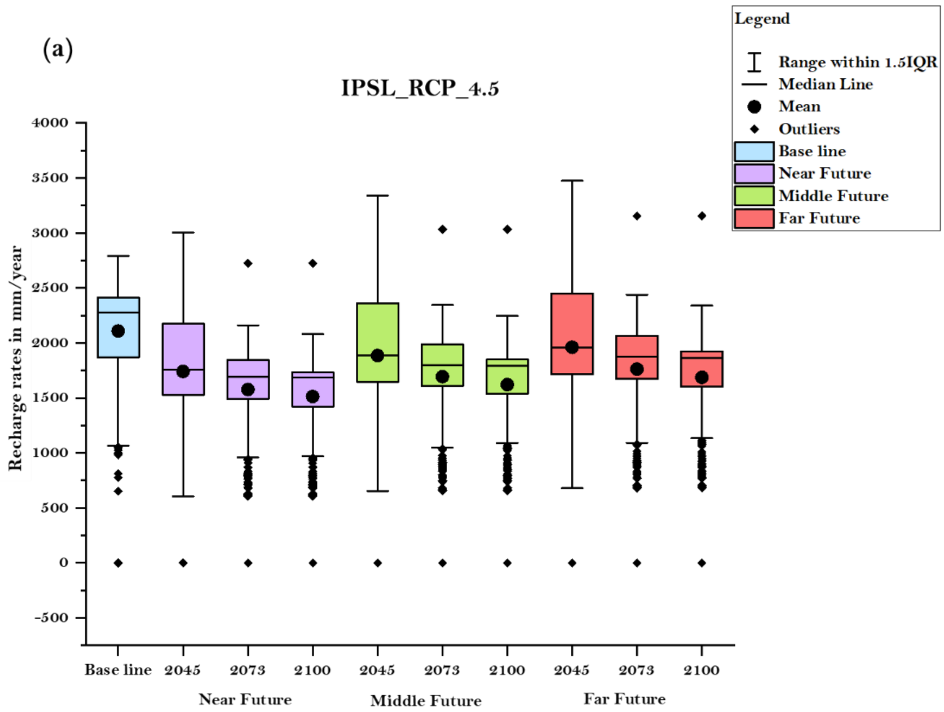

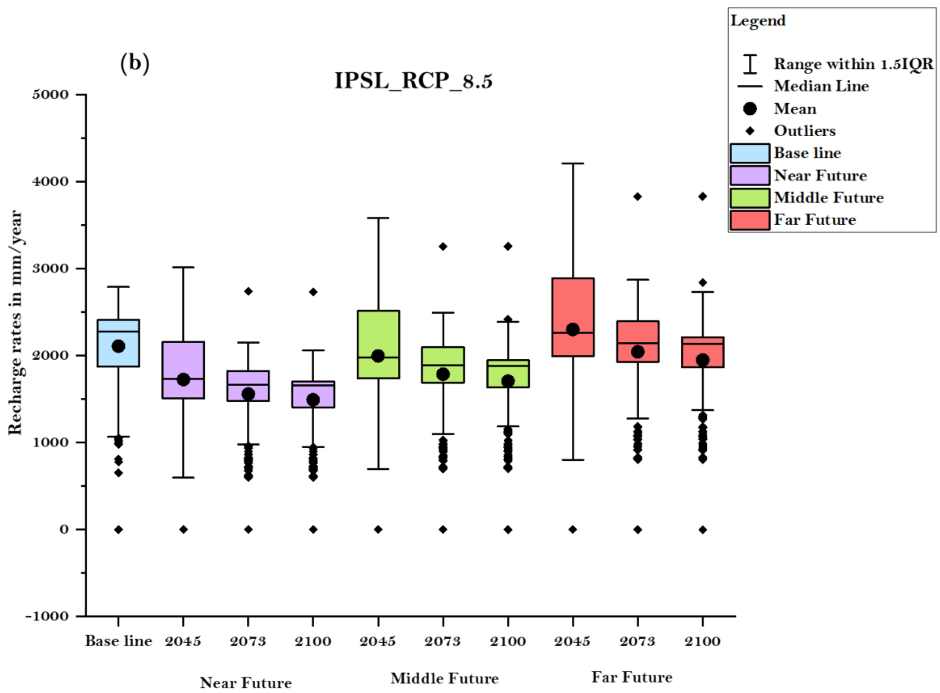

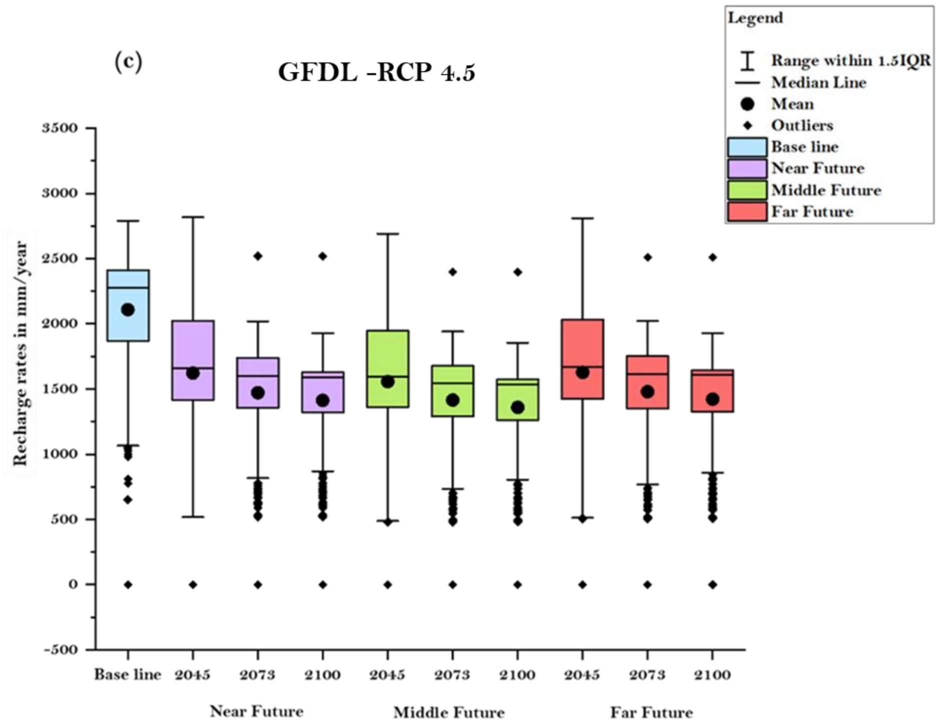

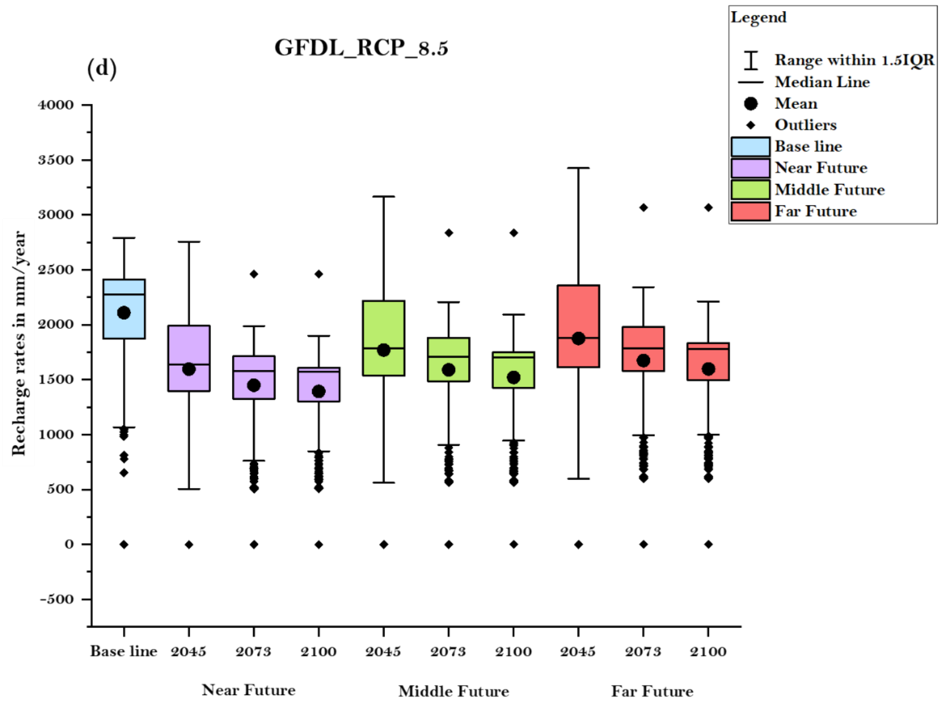

Figure 12 Comparison of average annual recharge rates for the Greater Cochin during three future phases: NF (2021-2045), MF (2046-2075), FF (2076-2100) with different LULC covers (2045, 2073, 2100) scenarios in respect to baseline recharge rates (1990-2020); (a) under IPSL-CM5A-LR_REGCM4-CM5A-LR_REGCM4 -RCP 4.5, (b) under IPSL-CM5A-LR_REGCM4-CM5A-LR_REGCM4 -RCP 8.5, (c) under GFDL-ESM2M_REGCM4-ESM2M_RegCM4- RCP 4.5 and (d) under GFDL-ESM2M_REGCM4-ESM2M_RegCM4-RCP 8.5

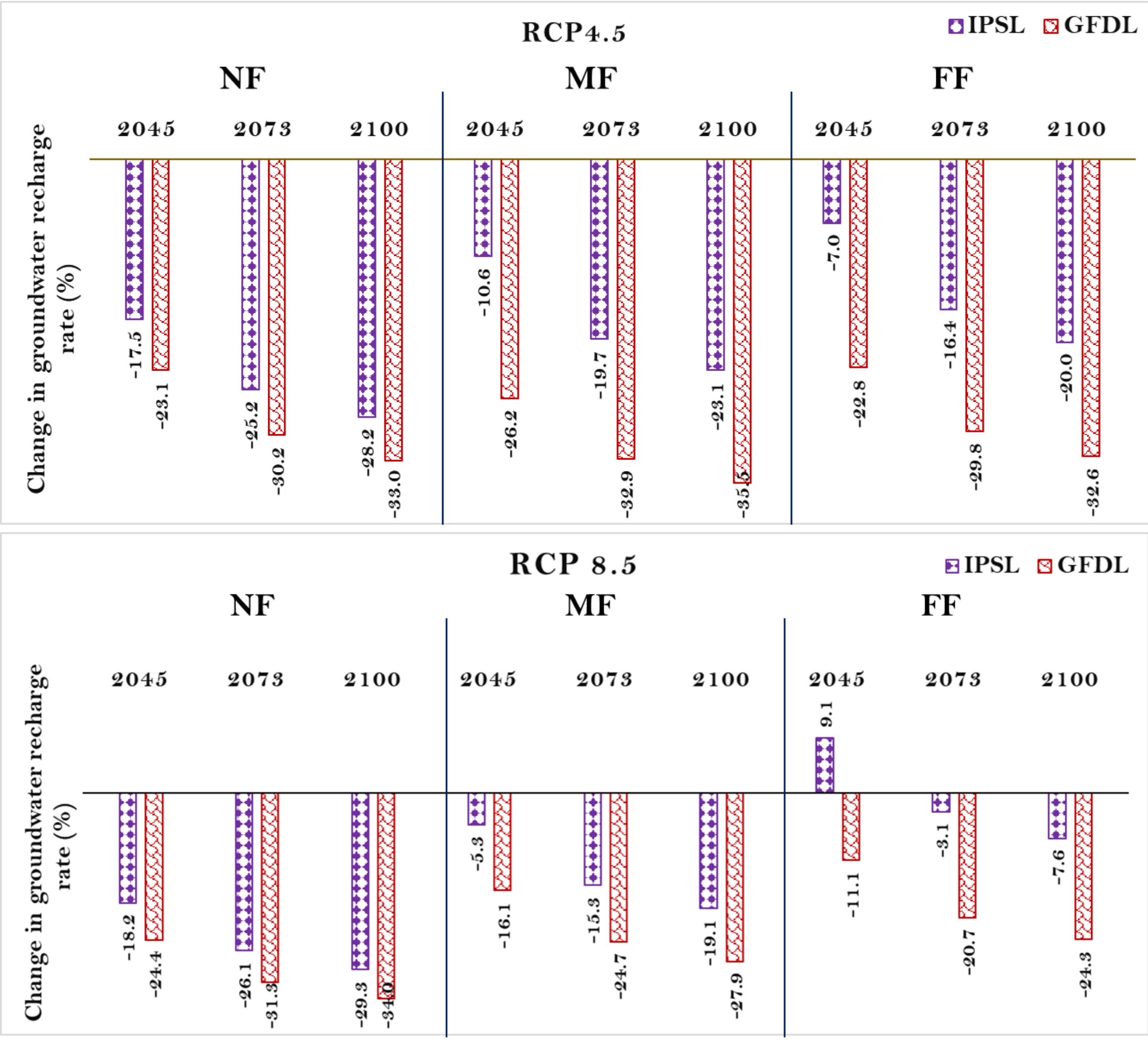

Figure 13 Change in future groundwater recharge rate from the baseline groundwater recharge rate for three different LULC (2045, 2073, 2100) and climate change (NF, MF, and FF) under (a) RCP 4.5 and (b) RCP 8.5 scenarios.

Table 4 Sensitivity analysis, their range of variability and best fitted values of the parameters

SWAT hydrological Parameter	Parameter description	Parameter ranges	Fitted value
ALPHA_BF.gw (v)	Base flow alpha factor (1/days)	[0, 1]	0.7
GW_DELAY.gw (v)	Delay time for aquifer recharge (days)	[0,500]	250
GWQMN.gw (v)	Threshold depth of water in shallow aquifer required for return flow to occur (mm)	[0,5000]	2500
GW_REVAP.gw (v)	Groundwater "revap" coefficient	[0.02,0.2]	0.11
RCHRG_DP.gw (v)	Deep aquifer percolation factor	[0,1]	0.5
REVAPMN.gw (v)	Threshold depth of water in shallow aquifer required for "revap" or percolation to deep aquifer to occur (mm)	[0,500]	50
SOL_AWC ().sol (r)	Available water capacity of the soil layer	[-0.3,0.3]	0.12
SOL_K ().sol (r)	Saturated hydraulic conductivity (mm/h)	[-0.3,0.3]	0.12
ESCO.hru (v)	Soil evaporation compensation factor	[0,1]	0.9
CN2.mgt (r)	SCS runoff curve number	[-0.3 ,0.3]	0.069
CH_N2.rte (v)	Manning's "n" value for the main channel	[0.01, 0.3]	0.02
EPCO.hru (v)	Plant uptake compensation factor	[0,1]	0.7

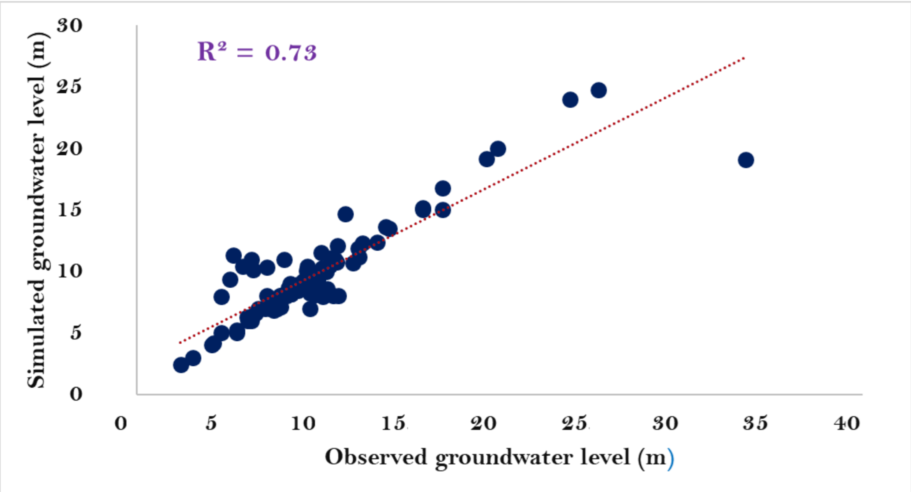

Figure 14 Correlation between observed and simulated steady state groundwater levels for the year 2015

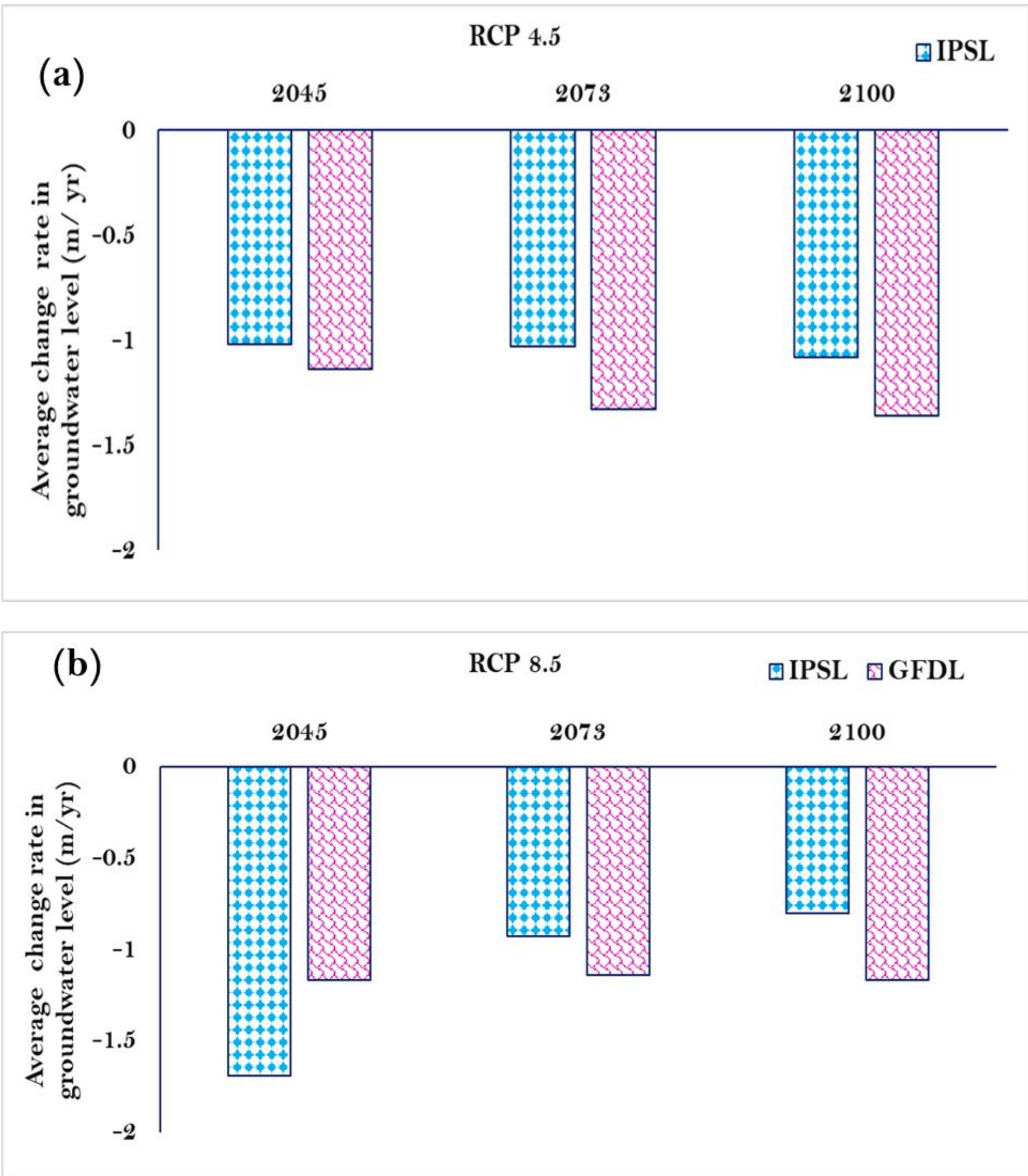

Figure 15 Relative average change rate in future groundwater level with respect to baseline condition for intervals :2045, 2073, and 2100 with respect to IPSL-CM5A-LR_REGCM4-CM5A-LR_REGCM4 and GFDL-ESM2M_REGCM4-ESM2M_REGCM4 under (a) RCP 4.5 and (b) RCP 8.5 scenario

1.3 Conclusions

This study utilised the SWAT model and simulation technique to evaluate the fluctuations in groundwater recharge rates forecasted for future projected LULC and climate conditions. To simulate the groundwater recharge rate for three projected LULC scenarios representing 2045, 2075 and 2100, the SWAT model set up used baseline observed climate data representing 1994 along with topography from DEM and soil data. For future climate projections, climate data from two regional climate models, IPSL-CM5A-LR_REGCM4-CM5A-LR_REGCM4 and

GFDL-ESM2M_REGCM4-ESM2M_RegCM4, were used for 4.5 and 8.5 RCP scenarios. The climate projection shows an increasing trend in both temperature and rainfall under RCP 4.5 and 8.5. The increase projected in T_{max} values ranges between 0.2 to 1.7℃ for the RCP 4.5 scenario and 0.5 to 2.42℃ for RCP 8.5. Also, the increase in forecasted Tmin ranges from 0.4 to 1℃ and 0.8 to 2.52℃ for RCP 4.5 and 8.5. The trend projected for the precipitation indicates an increase between 2.9 to 13% in RCP 4.5 and 6 to 35% in RCP 8.5. The GFDL-ESM2M_REGCM4-ESM2M_RegCM4 model projected the maximum rise in both Tmax and Tmin in RCP 8.5 scenarios.

LULC changes showed a high impact on the model simulated results. The projected groundwater recharge rates for 2045, 2073 and 2100 LULC with observed climate data of 1994 predicted a decreasing recharge trend of 20%, 27%, and 30%, respectively. Accordingly, the projected rate of reduction in groundwater recharge rate is relatively very high for the 2100 LULC scenario. For the highest urban expansion scenario of 2100 LULC, most of the study area is projected to modify as built-up, resulting in a substantial reduction of 30% in the average annual recharge rate. Thus, built-up as a land use class substantially affected groundwater recharge indicating the impact of surface imperviousness.

The study evaluated the combined impact of climate and LULC changes on the groundwater recharge rates. The near future climate scenarios projected a higher reduction in recharge rate compared to the middle and far future. In IPSL-CM5A-LR_REGCM4-CM5A-LR_REGCM4 climate model simulations, the groundwater recharge rate is projected to reduce by 18% for the near future RCP 4.5. The recharge rate may reduce to 19% under the RCP 8.5 scenario compared to the baseline. In the middle future, under RCP 4.5 and 8.5 scenarios, the reduction range between 20% and 15%, respectively. Far future projected a reduction of 20% in RCP 4.5 and 8% for RCP 8.5.

Similarly, for the GFDL-ESM2M_REGCM4-ESM2M_RegCM4 model, the groundwater recharge rate may reduce by 24% by the end of the near future in the case of RCP 4.5, while for RCP 8.5, the reduction is 24.4% to the baseline groundwater recharge rate. The reduction rates range between 33% and 25% under RCP 4.5 and 8.5 scenarios in the middle future. The far future showed a reduction in recharge between 33% and 24% for RCP 4.5 and 8.5 scenarios, similar to the middle future. Therefore, the reduction in groundwater recharge rate is drastic for the near future compared to the middle and the far future for both GFDL-ESM2M_REGCM4-ESM2M_RegCM4 and IPSL-CM5A-LR_REGCM4-CM5A-LR_REGCM4 models.